The Genetics of Idiopathic Intracranial Hypertension (IIH): Integration of Population Studies and Clinical Data

Roei Zucker[1], Michael Kovalerchik[1], Zvika Davidovich[2], Ehud Banne[3], Idit Maharshak[2,4], Michal Linial[5] *

[1]The Rachel and Selim Benin School of Computer Science and Engineering, The Hebrew University of Jerusalem, Jerusalem, Israel
[2]Department of Ophthalmology, Edith Wolfson Medical Center, Holon, Israel.
[3] The genetic Institute, Edith Wolfson Medical Center, Holon, Israel.
[4] Sackler School of Medicine, Tel Aviv University, Tel Aviv, Israel.
[5]Department of Biological Chemistry, Institute of Life Sciences, The Hebrew University of Jerusalem, Jerusalem, Israel

- Corresponding author: Michal Linial, Dept. of Biological Chemistry, Institute of Life Sciences, The Hebrew University of Jerusalem, Jerusalem, 91904, Israel; Phone: +972-54-8820035; Email: michall@cc.huji.ac.il

Running Title: Idiopathic intracranial hypertension and papilledema genetics

Abstract

Idiopathic intracranial hypertension (IIH) is a condition characterized by increased intracranial pressure without a known cause. It mainly affects overweight, reproductive-age women, and its genetic basis remains unknown. Previous GWAS failed to find significant associations. To address this, we analyzed a cohort of 173 IIH and papilledema (PAP) patients from the UK Biobank (UKB) using various genetic association methods. We activate a GWAS that covers only coding regions of genes for better interpretability. We also employed the complementary methods of SKAT and PWAS, which aggregate variants to determine gene-based association. We report on 10 overlapping genes by two methods, with FOXF1 and RGCC identified by all three methods. In a separate GWAS on a Finnish cohort, a rare variant in the LRRFIP1 gene was associated with IIH. Comparing findings from the Finnish, IIH, and PAP cohorts, we discovered the SHANK2 gene as a shared genetic factor. Genes related to the choroid plexus epithelium cluster (MAPK15, DCDC1, DNAH5, and SLC28A3) were found to be enriched, suggesting a role for microtubule cilia regulation in IIH etiology. Importantly, many GWAS-associated coding variants were predicted to be deleterious and rare in healthy populations. Comorbidities associated with IIH and PAP include pain, migraines, and psychological and mental disorders. This study highlights the strength of an integrative genetic approach, combining functional and clinical knowledge, to better understand IIH etiology. By identifying potential genetic factors and their biological relevance, this research provides insights into IIH's causes and paves the way for further investigation and potential therapeutic interventions.

Keywords:

Choroid plexus, GWAS, FinnGen, PWAS, SKAT, Cilia, papilledema, obesity, UK Biobank.

Introduction

Idiopathic intracranial hypertension (IIH, also called *Pseudotumor Cerebri*) is a condition of raised intracranial pressure (ICP) with no proven pathogenesis. It is linked to obesity, and patients are typically overweight women of reproductive age [1]. Common symptoms are headaches, transient visual obscurations (TVOs), pulsatile tinnitus, double vision, and neck pain. If left untreated, the disorder can lead to significant visual loss [2].

Diagnosis is usually based on the updated modified Dandy criteria [3], which necessitate the existence of a raised ICP, papilledema, and no identifiable secondary causes. In a study that compared cases with IIH and papilledema, only 5.7% of patients diagnosed with IIH did not have papilledema [4]. In the past, there was little evidence to guide the management of IIH, but significant prospective studies have contributed to our understanding of the disorder. Examples of such studies include the Idiopathic Intracranial Hypertension Treatment Trial (IIHTT), which examined the effects of the carbonic anhydrase inhibitor drug acetazolamide in patients with mild visual loss [5]. Additional studies tested the effect of a low-calorie diet on ICP and symptoms and signs of IIH [6]. Still, the pathogenic mechanisms of IIH are uncertain.

Dysregulation of ICP is an important direction of investigation. Three chief intracranial mechanisms have been proposed to cause raised ICP, including disorderly cerebrospinal fluid (CSF) dynamics such as CSF hypersecretion and outflow obstruction, and increased venous sinus pressure. In the past 5–10 years, several potential hormonal and metabolic causes of IIH have become known. Obesity is prominent in most cases of IIH, suggesting a strong link between the disorder and weight. One of the early theories proposed a physical effect of increased abdominal mass, raising intrathoracic pressure, and, as a result, increasing venous pressure [7]. This theory supported the improvement of the condition through weight loss. However, rendering this theory, one would expect to see a high number of overweight individuals, including men with the disorder [8], yet IIH affects women primarily [7]. Weight gain (i.e., 5–15% of total body weight) is linked to an increased risk of the development and reappearance of IIH in both obese and non-obese groups [9,10]. Patients who were not overweight (i.e., defined by the body-mass index [BMI] 25-30 kg/m²) stayed at risk after moderate weight gain, and this risk rose with percentage weight gain up to 15% [9].

Preliminary findings proposed an improvement in symptoms and signs of IIH with weight reduction [11]. This improvement was not established until investigators of a prospective cohort study [6] tested for significant improvements in ICP, papilledema, and headache after weight loss compared with a control period before weight loss. The mechanism by which weight loss improves IIH is uncertain. The effect of weight in terms of mass alone is a weak explanation because BMI and lumbar puncture opening pressure have a frail, non-significant relationship [12]. New metabolic therapeutic targets are emerging for IIH, the most hopeful being glucagon-like peptide 1 (GLP-1) receptor agonism [13]. GLP-1 receptor agonists (RAs) are extensively used in the treatment of type 2 diabetes mellitus (they do not cause hypoglycemia) and recently to manage obesity [14]. In the setting of IIH, the usage of GLP-1 RAs ranges beyond weight reduction. The GLP-1 receptor has been recognized to be expressed in human and rodent choroid plexus epithelium. When stimulated with the GLP-1 RA exenatide, it reduces CSF secretion. It has been shown that a morbidly high ICP can be lowered by nearly 50% in rats with intracranial hypertension treated with exenatide, with effects persisting over a week [15].

In addition to BMI, sex, age, ethnicity, and environmental factors (e.g., nutrition), we anticipate that the genetic landscape of individuals will affect their susceptibility to IIH and its comorbidity of vision

complications, specifically papilledema. Only a few studies addressed the underlying genetics of IIH. Due to the complex nature of the syndrome and its rarity, no causal variants were identified. Recently, GWAS analysis was performed on female patients from the IIHTT cohort (Idiopathic intracranial hypertension treatment trial) and their matched controls (95 women in each group). Altogether, from ~300K high-quality common SNPs, 15 associations were reported with weak statistics (p-values ranging from 1e-07 to 1e-05) [16]. No other genetic information is available, and testing either the group of patients with IIH (n=197) or papilledema in the FinnGene Fz8 (n=464) failed to report any significantly associated variant. Similar to other complex diseases, biological insight, and mechanistic interpretation are limited, as most variants are not assigned to any obvious causal gene [17].

In this study, we seek IIH/PAP genetics in the UK-BioBank by applying state-of-the-art gene-based approaches. The goal of this study is to identify genetic signals for IIH/PAP, and score candidate genes that are significantly associated with these conditions. We also analyzed the comorbidity of IIH/ PAP and we discuss the impact of current genetics and a medical record on patients' care.

Methods

Data resource and processing

We used the UK-Biobank (UKB) database for identifying the individuals with the selected ICD-10-CM (International Classification of Diseases, Tenth Revision) classification, using main or secondary diagnoses fields (UKB data fields 41202 and 41204, respectively). We restricted the analysis to ICD-10 combined phenotype of G93.2 (Benign intracranial hypertension and H47.1) and Papilledema. We used the genetic ethnic grouping, (data-field 22006) to remove genetic relatives, by randomly keeping only one representative of each kinship group.

For FinnGen Fz9 GWAS results we extracted the reported default analyses for the endpoints of IIH (called Benign intracranial hypertension, G6_BENINTRAHYP), and PAP (called Papilloedema, unspecified; H7_PAPILLOEDEMA). The inclusion and exclusion criteria and quality control used for the GWAS analysis are detailed at (https://risteys.finngen.fi/endpoints/). Note that the FinnGen relies on high imputation accuracy down to very low allele frequencies (AFs), which enabled the identification of associations with low-frequency variants using a routine GWAS approach. The high imputation accuracy combined with broad population registry-based phenotyping facilitates the identification of very low-frequency variants associated with rare phenotypes, which have largely been unused in GWAS.

Genetic Data

We tested 804,069 informative markers that were represented in our cohort. We considered only variants that are included in the 18,053 coding genes (including splicing variants). This set included the 639,323 coding genes imputed variants that were selected from the 97,013,422 whole genomes UKB imputed set. To select current knowledge from GWAS resources, we have used the Open targets genetic platform, (OTG, dated 3/2022) [18]. The OTG compiled information on any GWAS performed for IIH (EFO_1001132) and its synonyms (e.g., benign intracranial hypertension).

Association tests

We Performed three different association tests coined coding-GWAS, SKAT and PWAS. For all methods, we included 8 covariates including Sex, Year of birth, and the first 6 principal components to account for population structure.

Coding GWAS: GWAS (Genome-wide association study) is a common statistical method used to identify genetic variants statistically associated with a specific phenotype. A major caveat with this approach is the lack of Interpretability due to the difficulty of mapping variants to genes. Instead, we performed a restricted GWAS where the analysis covers variants in the coding regions of genes (accounts for ~1.5% of the genome). This allows greater Interpretability of the results since the connection of variant and function is plainer. We have used the accepted significant threshold for GWAS as p-values of <5e-08 and 5e-07 for whole genome and exome sequencing, respectively.

SKAT (Sequence Kernel Association Test): An additional limitation of any GWAS is that it considers individual variants as the only source for the association. While it is a powerful tool for examining the effect of a single variant, it fails to discover the accumulating effect of multiple variants on a phenotype. SKAT is a collapse-based association method that allows the estimation of the correlation of multiple variants to a phenotype at the same time. This approach both lowers the number of tests performed and thus lowers the statistical threshold required for significance, and allows to account for the combined effect of multiple variants according to the preselection of the relevant genomic information.

We performed a gene-based analysis using SKAT. The SKAT was applied to the same UKB-derived dataset (in particular, using the same covariates). We provided SKAT with the genotypes of all protein-imputed variants by the additive genotypes (i.e., the expected number of alternative alleles). We have used version 2.2.5 of the R package of SKAT (https://cran.r-project.org/web/packages/SKAT) [19], with output type for a dichotomous phenotype. As a default, we have used unweighted SKAT (β [1, 1]). For the gene-based SKAT, we only consider coding genes, therefore, we used as a significant threshold, the adjusted p-value of <0.05 following Bonferroni correction.

PWAS (proteome-wide association study): PWAS is another genetic analysis method, used for protein-level genetic analysis. Like SKAT, instead of performing an analysis for each variant individually, PWAS uses an aggregation method to analyze the genetic effect on phenotypes. Using the machine learning model of FIRM [20], the effect of each person's variants on protein function is estimated. PWAS aggregates the effect scores into a single score for each gene. For each person, each gene has a measurement for the variants' effect on gene function. To find the effect and significance of each gene's score on the phenotype, we used logistic regression. We ignore the models that were designed to address dominant or recessive heritability. The corrected p-value is by applying FDR <0.05 of the p-values.

Functional enrichment

We have used the Enrichr KB platform [21] to identify the genes that are significantly connected to GWAS terms and HPO terms with 1737 and 1779 terms, respectively. GWAS data covers 19,378 genes, and HPO reports on 3096 genes. We only considered the top 10 results for each GWAS report as candidate genes for the knowledge-based representation. Enrichr uses hypergeometric consideration for p-value and its adjusted value by correcting for multiple hypotheses. A combined score is reported by multiplying log(p-value) and z-score derived from the deviation from expectation. For gene expression analysis in the developing brain, we used FUMA [22]. STRING was used for functional enrichment by applying a high connectivity threshold (0.7). FUMA-GWAS was used by default parameters for functional enrichments from a list of genes and all coding genes as background [22].

Results

IIH from the UK-biobank (UKB)

Large population cohorts are routinely used for studying common complex diseases and human traits. In this study, we address the rare phenotype of IIH by genetic association and testing IIH comorbidities. We revised the utility of case-control settings from the large populations of UK Biobank (UKB) to highlight candidate genes to infer genetic signals underlying IIH. A substantial number of patients with IIH may also suffer from unspecified papilledema (PAP), we inspected both related conditions. We have compiled from the UKB individuals that were diagnosed with idiopathic intracranial hypertension (IIH, ICD-10: G93.2) and unspecified papilledema (PAP, ICD-10: H47.1).

Table 1 summarizes the demographic statistic of IIH and PAP diagnoses. We considered individuals of European origin, after excluding genetic relatives, and poor genotyping data (see Methods). We created a group of IIH/PAP for further analysis (n=173). We observed a very significant overlap of these two rare diseases, with 9% having both diagnoses (IIH+PAP, n=16, hypergeometric test p-value = 1.471e-39). There are 60% of females in the IIH/PAP group and a higher fraction of females (81%) among the subgroup of overlapping diagnoses. Statistical tests for the fraction of females within the IIH group relative to the entire female population confirmed their enrichment (Mann-Whitney U-test, p-value: 0.0046). Similarly, females are enriched when IIH and PAP groups were compared (U-test, p-value: 0.0252). Interestingly, none of these tests were significant for males (Supplemental **Table S1**). We also observed that females are diagnosed at an earlier age (age 39.6 and 36.4 for IIH and PAP, respectively). The age of diagnosis in males is about 3 and 10 years later for IIH and PAP, respectively. Inspecting the subset of 16 individuals with both diagnoses (denoted as IIH+PAP) indicated that for the majority (11/16) the diagnosis was provided at the same time, while for 4 of the other 5 cases, IIH diagnoses preceded PAP. High BMI characterized both females and males. However, a significant difference in the distributions was observed (Supplemental **Fig. S1**).

Table 1. IIH/PAP cohort statistical properties

Measure	Group	Males	Females	Both
Number	IIH/PAP	70	103	173
	IIH	38	67	105
	PAP	35	49	84
	(IIH+PAP)	3	13	16
Age of diagnosis	IIH	42.50	39.60	40.00
	PAP	46.00	36.40	38.20
BMI (mean)	IIH/PAP	29.03	30.91	30.14
	IIH	29.21	32.25	31.15
	PAP	29.45	29.77	29.64
	(IIH+PAP)	36.22	33.61	34.10
BMI (s.d.)	IIH/PAP	4.94	6.70	6.10
	IIH	5.47	7.06	6.66
	PAP	5.60	5.55	5.54
	(IIH+PAP)	12.97	4.91	6.54

Association studies from large populations

We performed several protocols for the association studies to propose candidate genes for IIH. A GWAS for IIH was previously conducted with 95 patients diagnosed with IIH out of 190 participants from mixed

population origins. All 15 associations that were reported are below significance by GWAS standards (study ID GCST005688) [16].

Fig. 1 presents the overall analyses that were performed from large population sources. The present study focuses on participants from the UK Biobank (UKB) for applying coding GWAS and gene-based SKAT. We also report on results obtained from FinnGen Fz9, a representative data source for a well-phenotyped isolated population [23]. We revisit the results provided by FinnGen from GWAS for the endpoint outcomes of IIH and PAP.

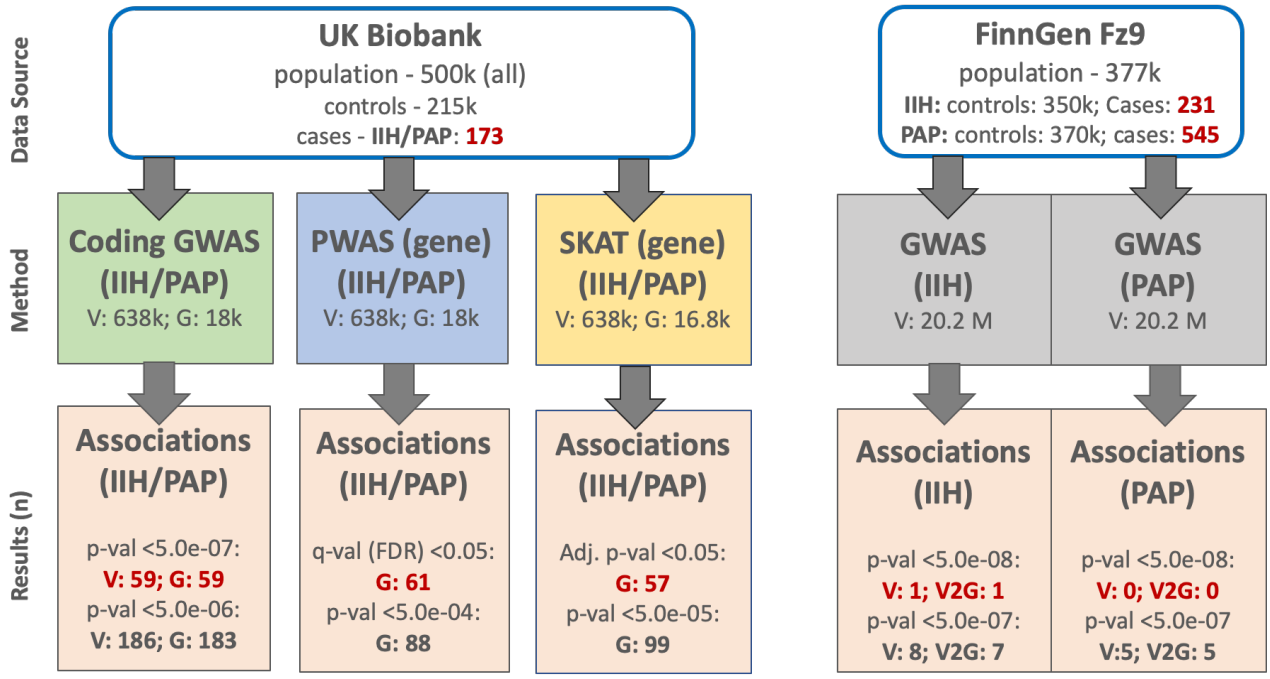

Fig. 1. A scheme for the data source and methods for identifying associations from the UK Biobank (UKB) and FinnGen Fz9 based on genotyping following imputation (see Methods). The reported numbers (in red) are discussed in the text. Note that for GWAS the threshold for significance is p-value <5.0e-08. For coding GWAS, we only consider the protein information within a gene (i.e., introns, 5'-UTR, and 3'UTR were excluded) with thresholds based on full exomes (p-value <5.0e-07) and a more relaxed one. For gene-based methods, the resulting p-value is adjusted by Bonferroni correction or by FDR in the case of PWAS according to the number of genes analyzed. V, variant; G, coding gene.

Coding-GWAS for IIH/PAP group

We seek a genetic effect associated with the complex condition of IIH/PAP as a unified group. To this end, we performed GWAS using only the coding regions (i.e., the RefSeq transcript of a gene that is included in the protein) to identify associated coding variants for IIH/PAP. **Table 2** lists the most significant variants (p-value <5.0e-9) identified by the coding GWAS approach along with the allele frequency (AF in %, extracted from gnomAD) and the impact on the associated protein. Note that in all cases (exception is FGFR1), the AF is below 0.1%, for the alternative (Alt) variant. We report on 183 significant genes (from 186 variants, p-values <5.e-06) in Supplemental **Table S2**.

Table 2. Properties of the most significant coding-GWAS variants

ID	Ref	Alt	P-value	AF (%)	Gene	Name	Protein: consequence
rs146069306	A	G	5.13E-11	0.0004	FOXF1	forkhead box F1	NP_001442.2: G160E
rs529730429	G	T	9.89E-11	0.0004	ZSWIM4	zinc finger SWIM-type containing 4	NP_001354763.1: L979R
rs775238614	CA	C	1.33E-10	0.03	PCDH15	protocadherin related 15	NP_149045.3: C1663fs
rs573651175	A	G	3.74E-10	0.0032	SPNS2	sphingolipid transporter 2	NP_001118230.1: R386H
rs200220130	T	G	4.43E-10	0.0304	ATF6	activating transcription factor 6	NP_031374.2: G6E
rs377424288	A	G	4.98E-10	0.007	RGCC	regulator of cell cycle	NP_054778.2: E26K
rs200588575	G	A	7.35E-10	0.0178	CCSER2	coiled-coil serine rich protein 2	NP_061872.2: M334V
rs121908162	T	C	1.24E-09	0.0608	KIF1B	kinesin family member 1B	NP_001352881.1: T873I
rs200689421	C	T	2.20E-09	0.005	HRC	histidine rich calcium binding protein	NP_002143.1: H80R
rs148498055	A	G	3.35E-09	0.0012	CUZD1	CUB and zona pellucida like domains 1	NP_071317.2: Q497T
rs140545796	T	A	4.00E-09	0.015	TCAIM	T cell activation inhibitor, mitochondrial	NP_776187.2: Y88C
rs56234888	A	G	4.28E-09	1.3068	FGFR1	fibroblast growth factor receptor 1	NP_056934.2: P770S

Fig. 2A shows the effect size (OR) along with the p-values for the more significant associated 73 coding variants (p-values <1.0e-06). A small set of variants displayed significant statistics and an elevated risk for IIH/PAP (**Fig. 2A**, shaded area). STRING analysis for functional enrichment for the 183 associated genes showed a slightly significant protein-protein interaction (PPI) network (p-value 0.0132). However, no functional terms were significantly enriched. The resulting STRING network was partitioned into subclusters with the function of integrins (8 genes), calcium signaling / ER (5 genes), and two smaller clusters of secretion including insulin release, and axonal transport in the synapse (4 genes each, **Fig. 2B**). We anticipate that the underlying biology for IIH/PAP is complex and is likely not associated with a single pathway or process.

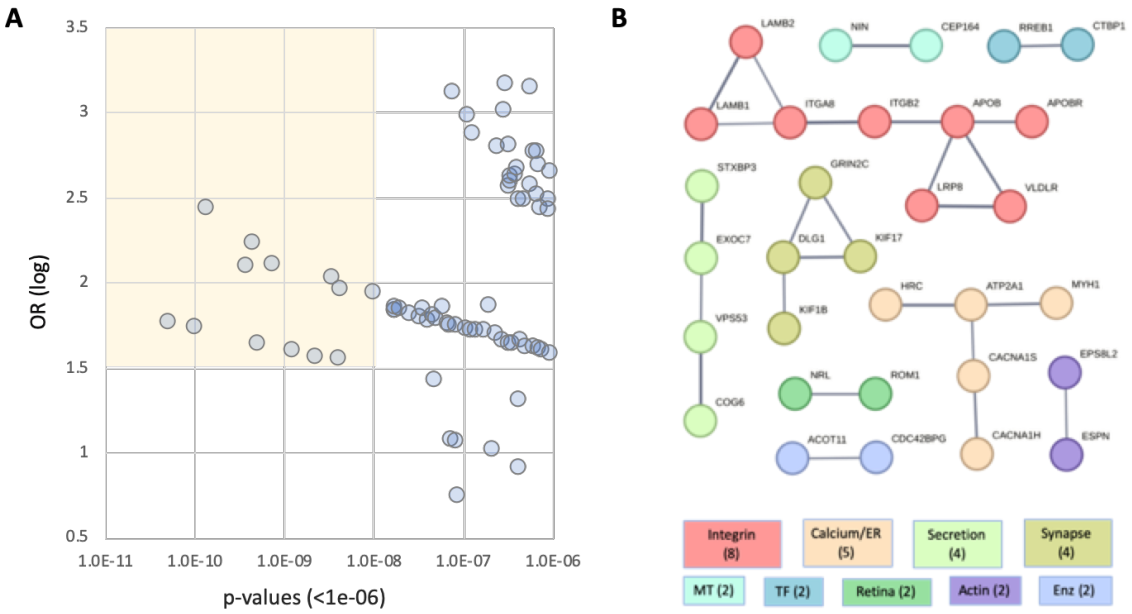

Fig. 2. Coding-GWAS associations to IIH/PAP**. (A)** Scatter plot of 73 genes with p-value <1.0e-06 along with the OR. Genes with maximal effect size and statistical significance are included in the shaded area. **(B)** A network graph based on STRING results for 183 significant genes (<5e-06) according to coding-GWAS for IIH/PAP group in the UKB. A STRING threshold of 0.7 was used. The PPI network includes 31 gene nodes and 25 edges (p-value 0.0132). The network is partitioned into colored clusters. Each subgraph is indicated with

its size and main functional property by a matched color. The rest of the genes were disconnected and are not shown. MT, microtubule; TR, transcription factor; Enz, enzyme.

GWAS for IIA and PAP based on the Finnish population

The size of the affected group (IIH/PAP) and the benefit of including extensive use of covariates for the UKB data [24] challenges the use of routine approaches. The cohort of FinnGen Fz8 (Dec 2022) included 197 IIH cases and 244,644 controls provided no reliable associations. However, the current release of FinnGen (Fz9, May 2023) was expanded to include 210,870 females and 166,407 males with 231 cases and 350,251 controls diagnosed with IIH. A single independent variant positioned at the end of the q-arm of chromosome 2 met the accepted GWAS threshold (<5e-08; Supplemental **Fig. S2**). Notably, the variant 2:237659125:G:A (rs545417105) is very rare in all populations, with allele frequency (AF) of 2.9e-04 in healthy Finnish and 1.6e-03 in non-Finnish Europeans. This top variant resides in the intron between exons 1 and 2 of the gene LRRFIP1 (Supplemental **Fig. S2**).

We tested the relevance of the leading variant associated with IIH (Chr2: rs545417105) with respect to all other phenotypes. To this end we applied PheWAS analysis [25] against 2272 phenotypic codes (**Fig. 3**). The most significant phenotypes are associated with an increased risk for IIH and PAP. The AF ratio of the alternative allele in cases and controls is 18.75 and 5.75 for IIH and PAP, respectively. We conclude that the rs545417105 is likely a causal candidate for IIH/PAP supporting a shared genetic effect that leads to IIH and PAP comorbidities.

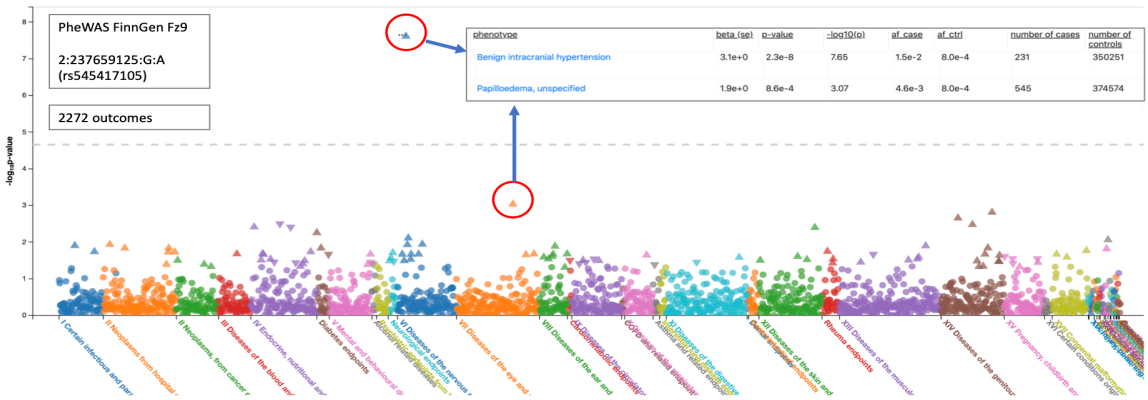

Fig. 3. PheWAS results for variant 2:237659125:G:A (rs545417105). The phenotypes (2272 codes) were clustered by their medical relevance. The triangle pointing up and down indicate an increase or decrease in the risk for the relevant disease, respectively. The statistical evidence is shown in the inset.

FinnGen Fz9 includes 545 cases and 374,574 controls for papilloedema, unspecified (PAP). Nevertheless, none of the variants reached statistical significance. The exception is two variants that are very close to the threshold: Chr8:75365414:A:G (rs144064178; p-value 6.12e-8), and Chr 4:162403766:T:C (rs1235196153; p-value 6.7e-8) (Supplemental **Fig. S3**). The variant in Chr 8 is rare (AF 0.7%), and in Chr4 is ultra-rare and was not detected in gnomAD 2.1. It is estimated to have an AF ranging from 8.5e-5 to 1.4e-4 across populations. These properties propose that this might be a causal variant for PAP (Supplemental **Fig. S3**).

Gene-based associations using SKAT and PWAS analyses

To improve the biological interpretation of the associations, we applied SKAT as a gene-based association method but restricted the analysis to coding regions based on the UKB genotyping imputed set (total, ~640k variants). SKAT resulted in 57 genes that were reported as significant (Bonferroni adjusted p-value <0.05, **Fig. 1**). In addition, we applied PWAS (see Methods) which resulted in 61 significant q-value <0.05. The ranked 15 genes of each method are listed in **Table 3**. We observed a quarter of these most significant genes also to be relevant to OMIM monogenic diseases. According to the Open Targets (OT), each gene is listed for all genetic-associated traits. The nature of the most significant trait is indicated (**Table 3**). Note that two of the top genes are shared between the two methods (FOXF1 and RGCC)

Table 3. SKAT and PWAS -the top 15 associated genes for IIH/PAP group from UKB

Symbol	Rank (S, P)[a]	Gene name	Adj. p-value(S)	# of traits[b]	Top trait[c]	OMIM (ID)
NOVA2	S1	NOVA alternative splicing regulator 2	3.00E-52	M	Brain	618859
FOXF1	S2, P2	forkhead box F1	5.10E-36	H	Vasc	265380
NME2	S3	NME/NM23 nucleoside diphosphate kinase 2	1.30E-22	M	Phys	
RGCC	S4, P1	regulator of cell cycle	1.60E-22	M	Bone	
NRL	S5	neural retina leucine zipper	2.70E-17	M	Eye	613750
DEFB104A	S6	beta-defensin 104	3.30E-13	L	Brain	
CALML3	S7	calmodulin like 3	1.20E-10	M	Brain	
TPRKB	S8	TP53RK binding protein	1.30E-10	L	Brain	617731
VRK3	S9	VRK serine/threonine kinase 3	5.10E-09	-	-	
LSM11	S10	U7 small nuclear RNA associated	4.00E-08	H	Brain	619486
CDR2	S11	cerebellar degeneration related protein 2	6.00E-08	M	Phys	
ACP1	S12	acid phosphatase 1	1.80E-07	H	Vasc	
PLCXD3	S13	phosphatidylinositol specific phospholipase C X domain containing 3	5.50E-07	L	Phys	
HEXIM2	S14	HEXIM P-TEFb complex subunit 2	8.40E-07	H	Phys	
XKR6	S15	XK related 6	1.10E-06	H	Phys	
RBAK	P3	RB associated KRAB zinc finger	1.95E-04	M	Heart	
H2AP	P4	H2A.P histone	7.25E-04	M	Eye	
BCL2L2	P5	Bcl-2-like protein 2	9.15E-04	H	Phys	
ORC5	P6	origin recognition complex subunit 5	9.15E-04	M	Brain	
FUNDC2	P7	FUN14 domain containing 2	2.57E-03	L	Blood	
UBE2D3	P8	ubiquitin conjugating enzyme E2 D3	2.57E-03	H	Blood	
ZNF639	P9	zinc finger protein 639	2.57E-03	L	Blood	
MRPS6	P10	mitochondrial ribosomal protein S6	2.69E-03	H	Mix	
CLDN25	P11	claudin 25	3.80E-03	H	Mix	
TRAPPC2	P12	trafficking protein particle complex subunit 2	4.46E-03	M	Phys	313400
TWIST2	P13	twist family bHLH transcription factor 2	4.46E-03	H	Skin	227260
ENAH	P14	ENAH actin regulator	5.16E-03	H	Mix	
CTNNBIP1	P15	catenin beta interacting protein 1	5.52E-03	M	Blood	

[a]Rank by statistics of PWAS (P) and SKAT (S). [b]According to OT, the number of genetic-associated traits partitioned to low (L:1-2), medium (M:3-10), and high (H:>11). [c]A broad-sense phenotypes based on OT. Phys, physical measurements (e.g., BMI); Vasc, vascular diseases; Brain, neurological/mental condition.

Inspecting the gene lists associated with IIH/PAP according to SKAT and PWAS showed that the lists are not particularly enriched in any specific function or indicated a relevance to the clinical manifestation of IIH or PAP. The most significant gene (q-value: 3.0e-52) is NOVA2 (Neuro-oncological ventral antigen 2, **Table 3**). NOVA2 acts during CNS development to regulate alternative splicing in neurons. It is noted that by regulating splicing, NOVA2 determines vascular morphogenesis and endothelial biology [26]. NOVA2 was also detected by PWAS (ranked 54 of 61). Inspecting the knowledge associated with the listed genes by OT showed that many of the genes (**Table 3**) contributed to the genetic basis of physical measurements (e.g., BMI), brain measurements, and unspecified clinical relevance (i.e. mix). For example, the NME2, CALML3, and ACP1 are reported to have genetic associations with body measurements (i.e., BMI, fat body mass). RGCC and LSM11 are associated with different traits of blood pressure and brain measurements, and DEFB104A is associated with neuroticism **(Table 3).** All significant genes identified by SKAT and PWAS are listed in Supplemental **Table S3** and **Table S4**, respectively.

To increase physiological interpretability, we focused on data integration. While all compared methods (coding GWAS, PWAS, and SKAT) use the same set of variants, the underlying model for identifying association is substantially different. Firstly, we sought gene overlap between the genes listed by SKAT, PWAS, and coding-GWAS (**Fig. 4A**). We identified FOXF1 and RGCC genes that were also among the most highly significant genes. We, therefore, suggest a direct association of these genes with the clinical phenotype of IIH/PAP. In addition, there were 5 genes that were shared between the SKAT and PWAS and another 5 between the coding GWAS and SKAT. Among the shared genes of coding GWAS and SKAT are LSM11 which leads to defects in chromatin structure and a causal gene for Aicardi-Goutieres syndrome 8 (AGS8) disease, and SLC28A3 which is Involved in the homeostasis of endogenous nucleosides. Among the shared genes of PWAS and SKAT, we identified BARX2, a gene that controls the expression of neural adhesion molecules such as L1. The CLDN25 gene plays a major role in tight junction-specific obliteration of the intercellular space, and NME2, which indirectly affects mitochondrial fragmentation.

Fig. 4B shows a Venn diagram for the top results retrieved from FinnGen Fz9 GWAS for GWAS and the IIH and PAP. Recall that the FinnGen listed genes failed to meet the GWAS confidence threshold and thus are considered a noisy list. Moreover, the associated genes are the genes closest to the lead variant. Evidently, mapping from variant to gene is dependent on the presence of independent evidence from chromatin structure, gene expression, and more [27]. SHANK2 is the only gene shared by GWAS of IIH and PAP. A single lead variant occurs in the intron, thus an impact on protein function cannot be drawn. SHANK2 plays a role in postsynaptic scaffolding, and alteration in its regulation is a known predisposition to autism or mental retardation. In addition, MALT1 was identified as a shared gene for the top results of IIH association in FinnGen Fz9 and coding GWAS. The gene function is mostly associated with adaptive and innate immune signaling. **Fig. 4C** shows the analysis of the SHANK2 variant for PheWAS association of all 2272 outcomes reported in FinnGene Fz9. The variant shows maximal association for IIH and PAP and several disorders of the optic nerve. Whether these results highlight the involvement of the immune system and brain synapse activity in the complex phenotype of IIH and PAP calls for future functional studies.

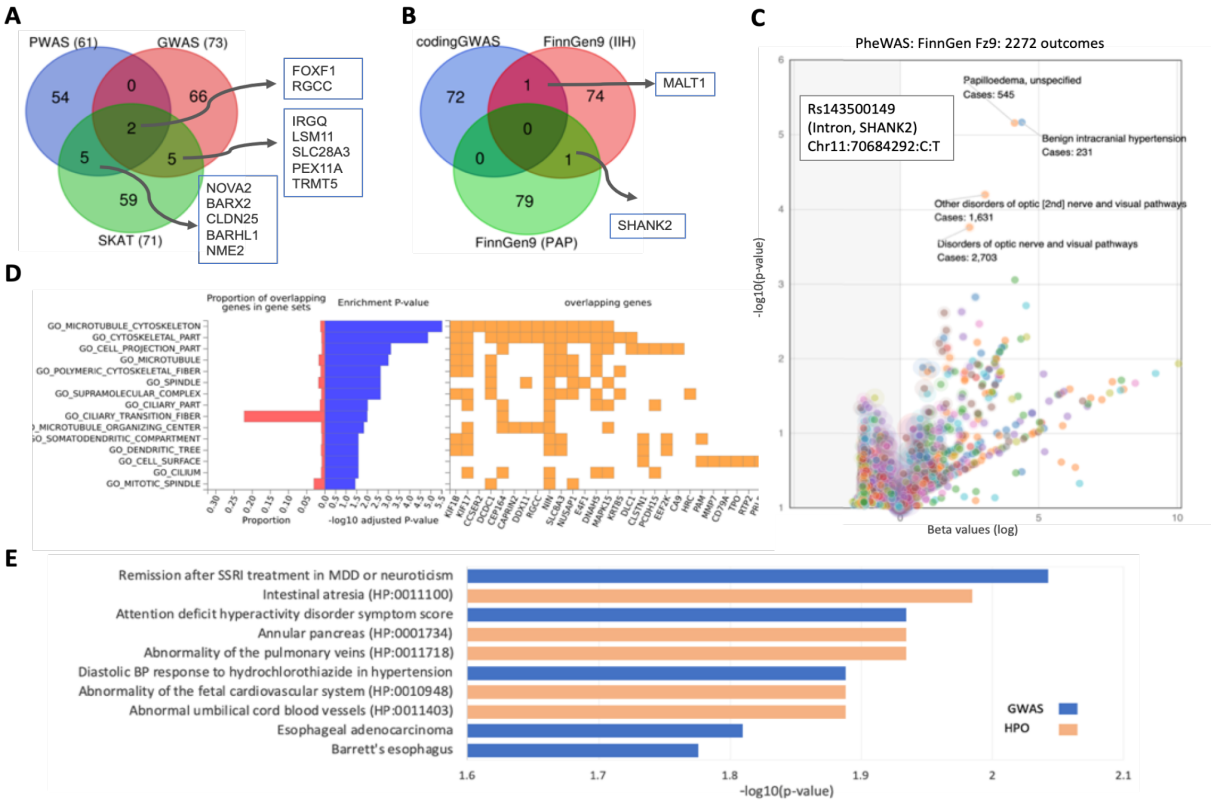

Fig. 4. Comparing IIH and PAP association results. **(A)** Venn diagram for the top results from SKAT (71 genes, p-value 1.0e-05), PWAS (61 genes, q-value <0.05), and coding GWAS (73, p-value <1.0e-06. **(B)** Venn diagram for the top results retrieved from FinnGen Fz9 (at a GWAS threshold of p-value <1.0e-05 for IIH (76 genes) and PAP (80 genes). **(C)** Volcano plot of PheWAS results of Rs143500149 variants at the intron of SHANK2. The most significant associations for all 2272 FinnGen outcomes are listed. The highest p-value accounts for the IIH and PAP as well as for broad diagnoses of disorders of the optic nerve (orange). The number of cases is indicated for each significant outcome. **(D)** Enrichment of the input genes from coding GWAS (59 genes, p-value <5.0e-07) by FUMA gene sets [27]. The proportion of overlapping genes that are shared (red) and the log10(p-value) of GO (gene ontology) cellular component indicate the dominant representation of cilia, microtubules, and cell projections. In orange, a subset of genes by their shared GO annotations. **(E)** Enrichment test for the 26 genes with an adjusted p-value <1.0e-4 by SKAT (Supplemental **Table 3**). The enrichment is according to EnrichR KB for all the results from the GWAS catalog (blue bars) and HPO (orange bars). Enrichment is indicated by the -log10(p-value) for the listed annotations.

Functional interpretation by external knowledge

Based on the negligible overlap among the associated genes **(Fig. 4B),** and the assumption that association methods suffer from a shortage in detection power, we used the enrichment schemes of FUMA-GWAS [27]. **Fig. 4D** summarizes the enrichment in GO annotation (cellular component) of the gene list input of coding GWAS (59 genes) [27]. The occurrence of the ciliary transition fiber annotation among the associated genes indicates the over-representation of cilia, microtubules, and cell projections. Some of the involved genes (**Fig. 4D,** right) such as NIN (ninein) propose a role for microtubules at the centrosome. **Fig. 4E** shows the results of Enrichr KB [21] for 26 genes with adjusted p-value <1.0e-4 identified by SKAT (Supplemental **Table S3**). By exploring the GWAS catalog and the human phenotype ontology (HPO) with >1700 terms in each resource (see Methods), a link to MDD and neuroticism was detected [28]. The gene of XKR6 was implicated

in treating MDD but it was also associated with physical measurements (BMI, diet measurements), and chronic metabolic diseases (systolic blood pressure, neuroticism, type 2 diabetes). Other traits include ADHD, retinal vascular caliber, and others. Terms that are linked to hypertension were identified to be enriched (e.g., abnormality of the pulmonary veins, diastolic BP, Fetal cardiovascular system, and abnormality in umbilical cord blood vessels; **Fig. 4E**). Supplemental **Fig. S4** shows the Enrichr KB for SKAT genes by a gene-centric network. Using external data sources suggests a clinical lead and functional insight into the genetics of IIH/PAP.

It is known that the choroid plexus epithelium is critical for the production, composition, and absorption of the CSF [29]. In seeking biological knowledge about the identified genes, we search for genes that act in the choroid plexus epithelium and focused on the 256 genes that have "tissue-enhanced" expression in the choroid plexus by Human proteome atlas (HPA) compilation [30]. Comparing the coding GWAS (59 variants, p-value <5.0e-07) with the set of choroid plexus genes identified four shared genes with the following variants: rs572968052 in DCDC1 (doublecortin domain containing 1), rs45495391 in MAPK15 (mitogen-activated protein kinase 15), rs185855852 in DNAH5 (dynein axonemal heavy chain 5), and rs141990386 in SLC28A3 (solute carrier family 28 members 3). The variants in the genes DCDC1 and MAPK15 and in DNAH5 are ultra-rare and are predicted to be damaging according to variant inference tools (e.g. Polyphen2). DCDC1, MAPK15, and DNAH5 all have microtubule-related functions, with MAPK15 and DNAH5 having an important role in cilia. Cilia in the choroid plexus were shown to have a role in CSF circulation, and their dysfunction leads to hydrocephalus [31]. Additionally, Mutated DNAH5 was shown to cause hydrocephalus in mice [32]. Enrichment of the GWAS results and with choroid plexus (hypergeometric test p-value 9.87e-03) argue for a role of cilia function in IIH and PAP.

Comorbidities with IIH

In seeking links to the clinical implication of IIH/PAP, we tested the occurrences of other clinical ICD-10 diagnoses. To this end, we collected ICD-10 associated with each patient. An extensive list of ICD-10 is available in Supplemental **Table S5**.

Table 4. IIH /PAP patients from UKB and comorbidities.

ICD-10	Disease name	p- value	Counts (n)
G93.2	**Benign intracranial hypertension**	0.0E+00	105
H47.1	**Papilledema, unspecified**	1.8E-282	84
R51	Headache	1.5E-30	48
Z86.7	Personal history of diseases of the circulatory system	7.0E-10	43
I10	Essential (primary) hypertension	7.9E-10	98
F32.9	Depressive episode, unspecified	9.2E-09	34
E66.9	Obesity, unspecified	1.7E-06	32
Z92.1	Personal history of long-term (current) use of anticoagulants	1.3E-05	31
E11.9	Type 2 diabetes mellitus, without complications	1.8E-05	32
K44.9	Diaphragmatic hernia without obstruction or gangrene	3.5E-04	37
K21.9	Gastro-oesophageal reflux disease without oesophagitis	1.0E-03	29
E78.0	Pure hypercholesterolaemia	1.1E-03	43
Z86.4	Personal history of psychoactive substance abuse	7.0E-03	42

Table 4 shows the ranked list of diseases in the UKB for patients with IIH and PAP. We list the comorbidities with high occurrences (n>30). The most significant diseases are obesity, headache, and essential hypertension. We also observed an enrichment of usage of anticoagulants, circulation problems, Type 2 diabetes, and depression. Comparing the finding to the independent cohort from the FinnGen outcome confined that the most significant overlapping diagnoses include obesity, migraine, hypertension, pain, and mental disorders. Interestingly, comorbidities with asthma, hypothyroidism, and immune-related diseases were more prevalent in the Finnish population.

Discussion

Epidemiological studies estimated that more than 90% of IIH patients are obese, and over 90% are women of childbearing age. Numerous factors (e.g., pregnancy, multivitamins, oral contraceptives, corticosteroids, or antibiotic use) that were proposed to be associated with IIH have been refuted by controlled studies [1]. While elevated blood pressure is commonly reported in obese people, it was proposed that it is unlikely that there is a direct association between arterial hypertension and IIH. We propose to benefit from the deep phenotyping data available in UKB and FinnGene to extract statistical clinical data on IIH/PAP comorbidities. To improve patient management, the treatment seems to require multiple experts in nutrition, neurology, and ophthalmology [33].

The goal of our study is to determine IIH variants/gene associations and shed light on the etiology of this complex, rare condition. It is evident that risk is associated with obesity in females at their fertility age. However, IIH can also occur in men, non-obese adults, older adults, and also in prepubertal children [34]. Additional etiologies were revealed, including the use of recombinant growth hormone and all-trans-retinoic acid, arguing that IIH and PAP may also result from developmental alterations [35 45]. Moreover, it was shown that the occurrence of IIH among family relatives is higher than the occurrence in the general population [36]. Indirect evidence for the role of genetics in the disease's etiology relies on the observation that IIH is much less prevalent among Asians. While it may reflect the huge difference in obesity prevalence (i.e., 33.5% in the USA compared to 3% in Japan for adult females), obesity may not be the major risk among Asians diagnosed with IIH [37]. While there may be a genetic etiology accounting for the ethnic disparities, no loci or causal genes were identified [38].

In our study, we applied several complementary association studies to different cohorts for identifying causal genes. According to the FinnGen expanded cohort study (Fz9), the gene LRRFIP1 was identified. It is a cytosolic DNA sensor that has been implicated in the innate immune pathway. Moreover, altered serum or CSF levels of certain cytokines and chemokines have been demonstrated in IIH patients. Such signatures showed conflicting results [39]. We have not detected a significant genetic immunological signature associated with IIH/PAP in UKB. Polymorphisms in LRRFIP1 positively correlate with body fat, abdominal fat, and CRP level. People carrying a missense rare allele in this gene (rs11680012) have 30% more abdominal adiposity relative to carriers of the major alleles [40].

Among the genes that showed some overlap by applying multiple genetic association methodologies (coding-GWAS, SKST, and PWAS), only two genes were shared by all. One of them is the gene RGCC that regulates cell cycle progression in response to DNA damage. It was proposed as a candidate cell cycle target for neuroprotection during the onset of Alzheimer's disease [41]. The second gene is FOXF1, a developmental gene that is among the most significant SKAT-identified genes **(Table 3)** and the top GWAS result (p-value 5.1e-11). The leading variant is ultra-rare (AF of 4e-06), with only one allele identified out of ~250K alleles

in gnomAD. The identified variant (rs146069306) causes a change (Gly160Glu), which is considered deleterious. FOXF1 is a transcription factor involved in major developmental processes. As a transcription factor, FOXF1 is a hub that regulates cell adhesion, migration, and mesenchymal cell differentiation. In addition, it is a causative gene for ACDMPV (alveolar capillary dysplasia with misalignment of pulmonary veins), a disorder affecting the development of the lungs and their blood vessels [42]. It is possible that, in some instances of IIH, the genetic basis is attributed to an early developmental alteration.

Our study revealed no single etiology for IIH/PAP. Instead, we propose a curated and ranked list of variants and genes that were revealed for IHH/PAP as candidates for further investigation. We can draw some general principles from the discovery of associated variants and genes: (i) Almost all variants that were identified by the coding GWAS approach are rare or ultra-rare. They are often associated with a deleterious prediction (e.g., rs146069306 in FOXF1, see **Table 2**). (ii) The only statistically confident IIH-associated variant that was identified by FinnGen Fz9 is rs545417105 within the intron of LRRFIP1. We confirm that it is strongly associated with IIH but (less significantly) with PAP (**Fig. 3**). This observation supports the notion of shared genetic effects between the two phenotypes. It was further supported by inspecting the SHANK2 intron variant. This rare variant shows a maximal association with IIH, PAP, and broader phenotypes of eye diseases (**Fig. 4C**). (iii) The choroid plexus is a network of capillaries whose primary function is to produce CSF. Dysregulation in CSF production or absorption can lead to IIH. Among the coding GWAS-identified variants, there are four overrepresented genes (MAPK15, DCDC1, DNAH5, and SLC28A3) expressed in the choroid plexus epithelium (hypergeometric test, p-value <0.01). An attractive role of these genes in cell mobility and cilia is manifested by MAPK15 (rs45495391, Gly36Ser), DCDC1 (rs572968052, Gly1315Glu), and DNAH5 (rs185855852, Arg661His). All these variants are very rare in the general population (AF <0.02%), suggesting that these rare variants may have a substantial effect size. The cilia of the choroid plexus are an important component of brain homeostasis [43]. We propose a genetic basis for the occurrence of affected individuals. (iv) Focusing on the coding region of genes (i.e., coding-GWAS, PWAS, and SKAT) leads to an immediate functional interpretation (stop gain, frameshift), and thus lend themselves better to causal explanations. Additionally, the impact of variants on the 3D protein structure can be modeled and the effect of rare variants on protein stability and the protein-protein interaction interface (e.g., [44]).

Functional inspection of the coding GWAS list (183 genes; p-value <5e-06) highlights a few genes that were associated with more than a single variant. These genes (TPO, MYH1, VRK3) have no sign of intolerance and thus may indicate cases of recessive inheritance for IIH/PAP [45]. Inspecting the SKAT and PWAS lists from a functional proteomics angle identified an overrepresentation of protocadherins (PCDH15, PCDHA1), which are known as cell adhesion proteins in the brain (enrichment factor 5.3 fold, p-value 0.007) and Claudins (CLDN25, CLDN3; p-value <0.01). Our study highlights the strength of utilizing integrative genetic and clinical approaches to gain a better understanding of the complex etiology of IIH. We claim that combining complementary association studies and including independent populations with knowledge-based methods has the potential to narrow down the most likely candidate genes. This approach will benefit personalized medicine in the rare instances of IIH and will lead to better disease management and treatment.

Abbreviations

BMI, body mass index; CSF, cerebrospinal fluid; ICD-10, International Classification of Diseases, 10th Revision; ICP, intracranial pressure; IIH, idiopathic intracranial hypertension; UKB, UK Biobank.

Data availability

All genotype-phenotype association data generated during this study are included in this published article and its supplemental information Tables. The individual-level genotype data are available under the restriction of the UK Biobank (UKB) Data Analysis Platform. The UKB application ID 26664 (Linial lab).

No custom code was developed for this project. We used in-house developed pipelines for the analytic procedures. The computational pipeline for processing the UKB data is open source and available at https://github.com/nadavbra/ukbb_parser (through both Python and a command-line interface).

Acknowledgments

We thank the reviewers for useful comments and suggestions. We thank the Linial lab for fruitful discussion. The study was partially supported by ISF grant 2753/20 (M.L.)

Supplemental Figures

Fig. S1. Distribution of BMI by sex.
Fig. S2. Manhattan plot and fine mapping of LRRFIP1 according to FinnGene Fz9 for IIH.
Fig. S3. Manhattan plot and fine mapping according to FinnGene Fz9 for IIH for PAP.
Fig. S4. Gene-based network of EnricR KB

Supplemental Tables

Table S1. U-test statistics for demographic data of Table 1.
Table S2. List of significant variants from coding-GWAS; source for Fig. 2.
Table S3. List of significant genes from SKAT; source for Table 3, Fig. 4.
Table S4. List of significant genes from PWAS; source for Table 3, Fig. 4.
Table S5. List of comorbidities; source for Table 4.

References

1. Wall M: Idiopathic intracranial hypertension. *Neurol Clin* 2010; **28:** 593-617.
2. Markey KA, Mollan SP, Jensen RH, Sinclair AJ: Understanding idiopathic intracranial hypertension: mechanisms, management, and future directions. *Lancet Neurol* 2016; **15:** 78-91.
3. Friedman DI, Liu GT, Digre KB: Revised diagnostic criteria for the pseudotumor cerebri syndrome in adults and children. *Neurology* 2013; **81:** 1159-1165.
4. Digre KB, Nakamoto BK, Warner JE, Langeberg WJ, Baggaley SK, Katz BJ: A comparison of idiopathic intracranial hypertension with and without papilledema. *Headache* 2009; **49:** 185-193.
5. Committee NIIHSGW, Wall M, McDermott MP *et al*: Effect of acetazolamide on visual function in patients with idiopathic intracranial hypertension and mild visual loss: the idiopathic intracranial hypertension treatment trial. *JAMA* 2014; **311:** 1641-1651.
6. Sinclair AJ, Burdon MA, Nightingale PG *et al*: Low energy diet and intracranial pressure in women with idiopathic intracranial hypertension: prospective cohort study. *BMJ* 2010; **341:** c2701.
7. Sugerman HJ, DeMaria EJ, Felton WL, 3rd, Nakatsuka M, Sismanis A: Increased intra-abdominal pressure and cardiac filling pressures in obesity-associated pseudotumor cerebri. *Neurology* 1997; **49:** 507-511.
8. Hannerz J, Ericson K: The relationship between idiopathic intracranial hypertension and obesity. *Headache* 2009; **49:** 178-184.
9. Daniels AB, Liu GT, Volpe NJ *et al*: Profiles of obesity, weight gain, and quality of life in idiopathic intracranial hypertension (pseudotumor cerebri). *Am J Ophthalmol* 2007; **143:** 635-641.
10. Ko MW, Chang SC, Ridha MA *et al*: Weight gain and recurrence in idiopathic intracranial hypertension: a case-control study. *Neurology* 2011; **76:** 1564-1567.

11. Kupersmith MJ, Gamell L, Turbin R, Peck V, Spiegel P, Wall M: Effects of weight loss on the course of idiopathic intracranial hypertension in women. *Neurology* 1998; **50:** 1094-1098.
12. Whiteley W, Al-Shahi R, Warlow CP, Zeidler M, Lueck CJ: CSF opening pressure: reference interval and the effect of body mass index. *Neurology* 2006; **67:** 1690-1691.
13. Mollan SP, Tahrani AA, Sinclair AJ: The Potentially Modifiable Risk Factor in Idiopathic Intracranial Hypertension: Body Weight. *Neurol Clin Pract* 2021; **11:** e504-e507.
14. Ghosh-Swaby OR, Goodman SG, Leiter LA *et al*: Glucose-lowering drugs or strategies, atherosclerotic cardiovascular events, and heart failure in people with or at risk of type 2 diabetes: an updated systematic review and meta-analysis of randomised cardiovascular outcome trials. *Lancet Diabetes Endocrinol* 2020; **8:** 418-435.
15. Botfield HF, Uldall MS, Westgate CSJ *et al*: A glucagon-like peptide-1 receptor agonist reduces intracranial pressure in a rat model of hydrocephalus. *Sci Transl Med* 2017; **9**.
16. Kuehn MH, Mishra R, Deonovic BE *et al*: Genetic Survey of Adult-Onset Idiopathic Intracranial Hypertension. *J Neuroophthalmol* 2019; **39:** 50-55.
17. Brandes N, Weissbrod O, Linial M: Open problems in human trait genetics. *Genome Biol* 2022; **23:** 131.
18. Ghoussaini M, Mountjoy E, Carmona M *et al*: Open Targets Genetics: systematic identification of trait-associated genes using large-scale genetics and functional genomics. *Nucleic Acids Res* 2021; **49:** D1311-D1320.
19. Wu MC, Lee S, Cai T, Li Y, Boehnke M, Lin X: Rare-variant association testing for sequencing data with the sequence kernel association test. *Am J Hum Genet* 2011; **89:** 82-93.
20. Brandes N, Linial N, Linial M: PWAS: proteome-wide association study-linking genes and phenotypes by functional variation in proteins. *Genome Biol* 2020; **21:** 173.
21. Xie Z, Bailey A, Kuleshov MV *et al*: Gene set knowledge discovery with Enrichr. *Current protocols* 2021; **1:** e90.
22. Watanabe K, Taskesen E, van Bochoven A, Posthuma D: FUMA: Functional mapping and annotation of genetic associations. *European Neuropsychopharmacology* 2019; **29:** S789-S790.
23. Kurki MI, Karjalainen J, Palta P *et al*: FinnGen provides genetic insights from a well-phenotyped isolated population. *Nature* 2023; **613:** 508-518.
24. Zucker R, Kovalerchik M, Linial M: Gene-based association study reveals a distinct female genetic signal in primary hypertension. *Hum Genet* 2023.
25. Denny JC, Ritchie MD, Basford MA *et al*: PheWAS: demonstrating the feasibility of a phenome-wide scan to discover gene–disease associations. *Bioinformatics* 2010; **26:** 1205-1210.
26. Belloni E, Di Matteo A, Pradella D *et al*: Gene Expression Profiles Controlled by the Alternative Splicing Factor Nova2 in Endothelial Cells. *Cells* 2019; **8**.
27. Watanabe K, Taskesen E, van Bochoven A, Posthuma D: Functional mapping and annotation of genetic associations with FUMA. *Nat Commun* 2017; **8:** 1826.
28. Amare AT, Schubert KO, Tekola-Ayele F *et al*: Association of the polygenic scores for personality traits and response to selective serotonin reuptake inhibitors in patients with major depressive disorder. *Frontiers in psychiatry* 2018; **9:** 65.
29. Praetorius J, Damkier HH: Transport across the choroid plexus epithelium. *Am J Physiol Cell Physiol* 2017; **312:** C673-C686.
30. Thul PJ, Lindskog C: The human protein atlas: a spatial map of the human proteome. *Protein Science* 2018; **27:** 233-244.
31. Banizs B, Pike MM, Millican CL *et al*: Dysfunctional cilia lead to altered ependyma and choroid plexus function, and result in the formation of hydrocephalus. *Development* 2005; **132:** 5329-5339.
32. Ibanez-Tallon I, Pagenstecher A, Fliegauf M *et al*: Dysfunction of axonemal dynein heavy chain Mdnah5 inhibits ependymal flow and reveals a novel mechanism for hydrocephalus formation. *Hum Mol Genet* 2004; **13:** 2133-2141.
33. Wakerley BR, Mollan SP, Sinclair AJ: Idiopathic intracranial hypertension: Update on diagnosis and management. *Clin Med (Lond)* 2020; **20:** 384-388.

34. Biousse V, Bruce BB, Newman NJ: Update on the pathophysiology and management of idiopathic intracranial hypertension. *J Neurol Neurosurg Psychiatry* 2012; **83:** 488-494.
35. Rangwala LM, Liu GT: Pediatric idiopathic intracranial hypertension. *Surv Ophthalmol* 2007; **52:** 597-617.
36. Klein A, Dotan G, Kesler A: Familial Occurrence of Idiopathic Intracranial Hypertension. *Isr Med Assoc J* 2018; **20:** 557-560.
37. Chen J, Wall M: Epidemiology and risk factors for idiopathic intracranial hypertension. *Int Ophthalmol Clin* 2014; **54:** 1-11.
38. Ghaffari-Rafi A, Mehdizadeh R, Ko AWK, Ghaffari-Rafi S, Leon-Rojas J: Idiopathic Intracranial Hypertension in the United States: Demographic and Socioeconomic Disparities. *Front Neurol* 2020; **11:** 869.
39. Altiokka-Uzun G, Tuzun E, Ekizoglu E *et al*: Oligoclonal bands and increased cytokine levels in idiopathic intracranial hypertension. *Cephalalgia* 2015; **35:** 1153-1161.
40. Mikhailova SV, Ivanoshchuk DE: Innate-Immunity Genes in Obesity. *J Pers Med* 2021; **11**.
41. Counts SE, Mufson EJ: Regulator of Cell Cycle (RGCC) Expression During the Progression of Alzheimer's Disease. *Cell Transplant* 2017; **26:** 693-702.
42. Dharmadhikari AV, Szafranski P, Kalinichenko VV, Stankiewicz P: Genomic and Epigenetic Complexity of the FOXF1 Locus in 16q24.1: Implications for Development and Disease. *Curr Genomics* 2015; **16:** 107-116.
43. Narita K, Takeda S: Cilia in the choroid plexus: their roles in hydrocephalus and beyond. *Front Cell Neurosci* 2015; **9:** 39.
44. Banne E, Falik-Zaccai T, Brielle E *et al*: De novo STXBP1 mutation in a child with developmental delay and spasticity reveals a major structural alteration in the interface with syntaxin 1A. *Am J Med Genet B Neuropsychiatr Genet* 2020; **183:** 412-422.
45. Lek M, Karczewski KJ, Minikel EV *et al*: Analysis of protein-coding genetic variation in 60,706 humans. *Nature* 2016; **536:** 285-291.